Research Article | Vol. 27, No. 8 | 15 Apr 2019 | OPTICS EXPRESS 11103
Optics EXPRESS

Broadly tunable femtosecond pulses around 2.06 μm from a diode-pumped Tm^{3+}-doped solid-state laser source

N. K. STEVENSON,[1,2,*] C. T. A. BROWN,[2] J. M. HOPKINS,[1] M. D. DAWSON,[1,3] AND A. A. LAGATSKY[1]

[1]*Fraunhofer Centre for Applied Photonics, Fraunhofer UK, Technology and Innovation Centre, Glasgow, G1 1RD, UK*
[2]*SUPA, School of Physics and Astronomy, University of St Andrews, St Andrews, KY16 9SS, UK*
[3]*Institute of Photonics, University of Strathclyde, Technology and Innovation Centre, Glasgow, G1 1RD, UK*
[*]*neil.stevenson@fraunhofer.co.uk*

Abstract: We report on a broadly tunable diode-pumped femtosecond Tm:$LuScO_3$ laser source around 2.06 μm. Tuning was obtained through the use of a steeply diving birefringent filter, maintaining sub-600 fs pulses over a tuning range of 2019–2110 nm. The minimum pulse duration of 240 fs was recorded at a central wavelength of 2080 nm with an average output power of 93 mW. Higher output coupling of 2% resulted in a narrower tuning range of 2070–2102 nm with generated pulses as short as 435 fs and an average output power of 119 mW at 2090 nm.

1. Introduction

Laser sources capable of generating high peak power ultrashort pulses in the ~2–2.1 μm spectral region are important for the development of new techniques and technologies in many fields from the mid-infrared photonics sector. Such sources can be used to efficiently access the deeper mid-infrared region through optical parametric frequency conversion techniques [1,2] or supercontinuum generation [3], enabling benefits to developments and applications in the areas of coherent X-ray sources [4], minimally invasive surgery [5], materials processing [6,7], and sensing [8]. The current laser amplifier systems required to achieve these high pulse energies tend to utilize Ho^{3+}-doped gain media such as Ho:YAG and Ho:YLF. The performance of these gain media have been widely reported in various amplifier configurations. However, the existing ultrashort pulse laser sources used to seed these amplifiers are rather complex. For example, the seed lasers used in [9–13] involve multiple nonlinear energy conversion schemes before a pulse covering a suitable spectral range is generated (Ho:YLF, 2050/2060 nm; Ho:YAG, 2090 nm). An alternative approach has been taken with the development of ultrashort pulse Ho:fibre lasers [14,15] which have been used to seed Ho:YLF amplifiers in single- [16] and multi-pass [17] configurations. Whilst such sources allow the seed optical spectrum to directly match the gain peak of Ho:YLF near 2050 nm, they require multiple pump stages with a Tm:fibre laser being involved. Commercially available Tm:fiber ultrashort pulse seed systems have also been coming to the market in recent years (Menlo Systems, InnoLas Photonics, and AdValue Photonics). While such fiber sources can offer a stable and turn-key operation, they struggle to operate efficiently at >2 μm wavelengths without some additional spectral shifting process and amplification stages to reach >100mW power level. These result in their high complexity and price.

#361041 https://doi.org/10.1364/OE.27.011103
Journal © 2019 Received 27 Feb 2019; revised 27 Mar 2019; accepted 28 Mar 2019; published 5 Apr 2019

Optics EXPRESS

A more efficient way to reduce the complexity and cost of these seed sources would be to develop an ultrashort pulse system that could benefit from direct diode-pumping whilst also being able to target the gain spectra of existing Ho:YAG and Ho:YLF amplifiers in the range of 2050–2100 nm. Recently it has been shown that Tm^{3+}-doped sesquioxide RE_2O_3 (RE = Lu, Sc, Y, or any $Lu_aSc_bY_c$ composition, where $a + b + c = 1$) gain media could support efficient laser operation at >2 μm wavelength under direct diode pumping [18]. In contrast to other Tm^{3+}-doped gain media, they possess ultrabroad and smooth gain features reaching the 2.1 μm spectral region avoiding strong water vapor absorption bands in the ~1800–2000 nm spectral range, which would prevent stable mode-locked operation. These features make Tm^{3+}-doped sesquioxides highly attractive for the development of compact and efficient femtosecond sources in the 2–2.1 μm spectral window, utilizing various mode-locking techniques and laser diode pump sources.

In particular, Tm:Lu_2O_3 has been reported in crystalline and ceramic forms to have produced sub-200 fs pulses near 2070 nm, employing a single-walled carbon nanotube saturable absorber [19] and an InGaAsSb quantum-well-based semiconductor saturable absorber mirror (SESAM) [20]. Employing the Tm:$LuScO_3$ crystalline gain media, we have previously demonstrated minimum pulse durations of 105 fs at 2010 nm [21]. More recently, the ceramic form of the mixed sesquioxide was reported to produce pulses as short as 63 fs at 2057 nm [22]. All of these systems were pumped using Ti:sapphire lasers operating around 800 nm. With the aim of making these systems more practical and less costly, laser diode pumping should be employed. However, the development of diode-pumped ultrashort pulse Tm^{3+}-doped lasers is not a straight forward process. Poor pump beam quality can lead to lower efficiencies, high thermal loads, Q-switching instabilities, and weaker self-phase modulation thus requiring precise cavity and saturable absorber engineering for stable mode-locking. In previous work [23], we reported on a diode-pumped Tm:Lu_2O_3 ceramic laser that generated pulses as short as 242 fs with an average output power of 500 mW at a central wavelength of 2068 nm and, more recently, a diode-pumped crystalline Tm:$LuScO_3$ laser capable of producing near-transform-limited 170 fs pulses at 2093 nm with an output power of 113 mW has been demonstrated [24].

Here we report on further development of diode-pumped ultrafast Tm^{3+}-doped sesquioxide lasers. In particular, broadly tunable femtosecond pulses spanning a >90 nm range around 2.06 μm from a diode-pumped, mode-locked Tm:$LuScO_3$ laser are demonstrated. With a 1% output coupler in use, a tuning range of 2019–2110 nm was achieved with an average output power as high as 96 mW and a corresponding pulse duration of 245 fs at 2090 nm. Under higher output coupling conditions of 2%, a maximum average output power of 119 mW with a corresponding pulse duration of 435 fs was achieved. Tuning of the femtosecond pulses was realized in a compact configuration through the use of a steeply diving birefringent filter (SD-BRF). To the best of our knowledge, this is the first use of such technique for the tuning of ultrashort pulses in the 2–2.1 μm region and paves the way for the development of compact, efficient, and versatile seed sources for the existing Ho^{3+}-doped laser amplifiers.

2. Steeply diving birefringent filter design

In the design of conventional BRFs the birefringent material is cut so that the optic axis runs parallel to the surface of the plate ($\theta = 90°$ in Fig. 1). Tuning of the laser emission wavelength can be achieved by rotating the plate around the surface normal, changing the angle of rotation (α). Assuming the plate is inserted into the cavity at Brewster's angle ($\beta_e \approx 57°$ for quartz at 2.1 μm), then the wavelength-dependent polarization changes due to the material's birefringence induce Fresnel reflection losses at the plates surfaces for the s-polarized component of the beam. This causes a wavelength dependent transmission loss as the plate is rotated. The thickness of the plate (t) defines the free spectral range (FSR) and the

Optics EXPRESS

transmission passband bandwidth; as the plate thickness increases, the FSR and transmission bandwidth decrease.

In the case of a SD-BRF, the birefringent material is cut in an orientation such that the optic axis dives into the surface of the plate, i.e. $\theta \neq 90°$. This has the effect of providing a larger FSR and transmission bandwidth for a given plate thickness compared with a conventional BRF. Tuning of the laser wavelength with a SD-BRF is achieved in the same way as a conventional BRF, except that in the case of the SD-BRF multiple separate orders with different transmission bandwidths at a particular wavelength exist at different angles α. When such SD-BRFs are applied to broadband mode-locked lasers, it can be seen that the ability is gained not only to set the emission wavelength but also coarsely control the optical bandwidth and thus, potentially the pulse duration of the pulse as previously demonstrated in Cr:LiSAF lasers [25,26]. Additionally, using a SD-BRF in combination with negative group delay dispersion mirrors allows construction of more compact and broadly tunable ultrafast lasers with improved robustness compared to those with prism based dispersion compensation schemes.

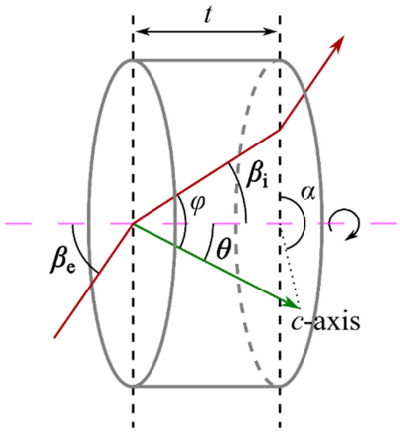

Fig. 1. Schematic illustration of a SD-BRF with light beam (red line) incident at Brewster's angle [27]. The optic axis (*c*-axis) is identified by the green line, while the pink dashed line indicates the surface normal. β_i, the internal Brewster's angle; θ, optic axis angle with respect to surface normal; φ, angle between the propagating beam and the optic axis.

The theoretical analysis of the SD-BRF has been reported previously with the aim of providing optimal design parameters for broadband tunability [27,28]. For instance, in [27] Demirbas proposed that the optic axis angle θ of 25° ± 2° is optimum for quartz, while Naganuma *et al* state that, due to the minimal change in refractive index from 0.5 to 2 µm, a near 24° angle is suited for any required wavelength within the range. For our work, an optic axis angle of 24° and a thickness of 2.7 mm were chosen and used for modelling the BRF performance in the 2–2.1 µm region using the approach taken in [25]. The thickness was chosen to give an optimized balance between transmission bandwidth and transmission contrast for a target wavelength of 2090 nm.

Figure 2(a) shows the transmission curves for the first four orders of our SD-BRF. It can be seen that the 1st order, shown in red at a center wavelength of 2090 nm for a rotation angle α of 28.2°, has the largest bandwidth, followed by the 2nd in green, the 3rd in blue, and the 4th shown in orange. All four orders provided similar transmission contrast. As only a small percentage of the introduced loss by the BRF is required to force the laser to operate at the intended wavelength and bandwidth, 1% or less, it is more practical to consider the 99% transmission bandwidths as was done in [25]. As such, the calculated 99% bandwidths were 28 nm, 14 nm, 9 nm, and 7 nm for the 1st–4th orders, respectively [Fig. 2(b)]. Figure 2(c) shows tuning spectra using the 1st order of operation. Tuning from 2028 nm to 2123 nm from

Optics EXPRESS

only 1° degree of rotation can be achieved, giving a predicted tuning rate of 95nm/° for this case.

3. Diode-pumped tunable femtosecond Tm:$LuScO_3$ laser

Initial characterization of the Tm:$LuScO_3$ laser with SD-BRF was performed in the continuous wave (CW) regime. A diode-pumped Tm:$LuScO_3$ laser similar to that reported in [24] was constructed (Fig. 3). In anticipation of moving into the mode-locked regime at a later point, the z-fold six mirror cavity was setup to operate in stability region II, producing a second waist of 130 µm in radius on the end HR-mirror in the short arm of the cavity. Additionally, the long arm of the cavity featured a 1% output coupler (OC) and contained two HR-coated Gires-Tournois interferometer (GTI) mirrors (GTM1 and GTM2) which provided a total round-trip dispersion of ~-3840 fs^2 (at 2095 nm). Two HR-coated, 75 mm radius of curvature folding mirrors (M1 and M2) created a waist radii of 26 µm × 24 µm inside the plane-plane, 4 mm long, 3 mm × 3 mm in aperture, AR-coated, 4 at.% Tm:$LuScO_3$ laser crystal (LC). The crystal was mounted onto a heatsink maintained at 20°C. It is estimated that the gain medium and SD-BRF introduced an additional round trip dispersion of –298 fs^2 and –741 fs^2, respectively. The pump beam was characterized and found to have a beam quality factor of 18 and 1.3 in the *x* and *y* directions, respectively. Focusing into the LC using a 100 mm focal length achromatic doublet lens (L), the pump waist radii were measured to be 54 µm × 22 µm. Pump optics were chosen so that the cavity and pump waists achieved the best possible overlap within the gain medium. All HR mirrors used were designed with reflectivity >99.9% in the range 1836–2176 nm, while the GTI mirrors were coated for 1915–2140 nm having similar reflectivity characteristics.

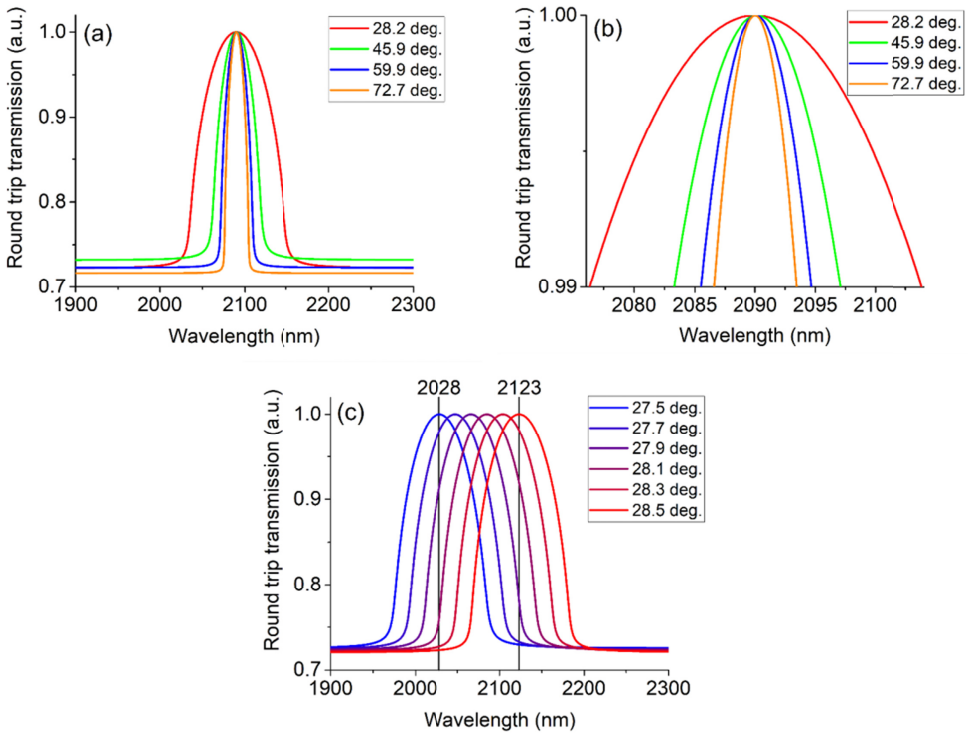

Fig. 2. (a) Modelled transmission curves for the first four orders of the SD-BRF at different angles *α*. A zoomed in view detailing the 99% transmission is shown in (b). (c) Change in transmission wavelength for the 1st order over various *α*.

Optics EXPRESS

With the quartz SD-BRF inserted into the cavity at Brewster's angle and under 1.8 W of incident pump power at 793 nm (1.2 W absorbed power), output wavelength tuning extending from 1986 nm to 2140 nm was obtained (Fig. 4). From these data, it can be seen that all four SD-BRF orders have a very similar profile indicating that the different orders were capable of supporting the same tuning range and that the BRF was operating as designed. It is believed that the tuning range shown here is limited only by the available gain of Tm:$LuScO_3$ around 2.06 µm at the given pump power level.

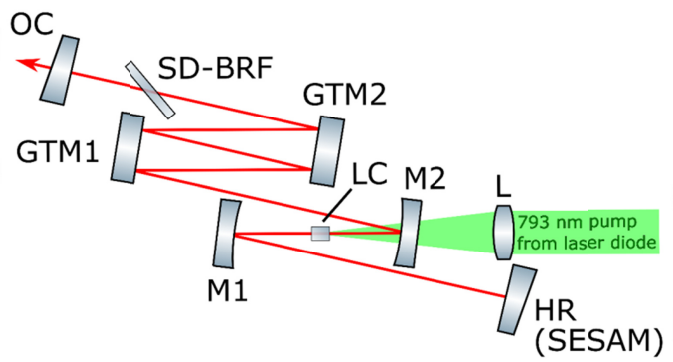

Fig. 3. Schematic of the z-fold six-mirror cavity used to demonstrate broad tunability around 2.06 µm from the Tm:$LuScO_3$ laser. When operating in the mode-locked regime, the HR mirror was replaced with a SESAM. Details of the pump source and optics used can be found in [24].

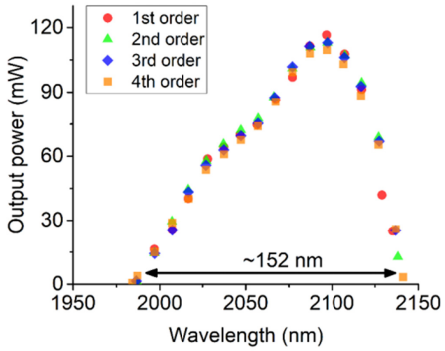

Fig. 4. CW tuning of the Tm:$LuScO_3$ laser over the first four orders of the SD-BRF.

Moving to the mode-locked regime involved firstly removing the SD-BRF and replacing the short arm end HR mirror with an ion-implanted InGaAsSb quantum-well-based SESAM. The SESAM device was designed to support mode-locked operation over a large optical range and was characterized by a low-signal reflection of 99.5% at 2 µm which gradually reduces to 98.1% at 2.1 µm. The corresponding modulation depth and nonsaturable loss parameters were estimated to be 0.3–1% and 0.2–0.9%, respectively, in the 2–2.1 µm range [29]. Once the SESAM was aligned, self-starting, single pulse, stable mode-locked operation was achieved. A minimum pulse duration of 173 fs (assuming a $sech^2$ intensity autocorrelation profile) was measured with an average output power of 128 mW. The pulse had a central wavelength of 2093 nm and optical bandwidth of 26.8 nm at the full-width at half-maximum (FWHM).

The SD-BRF was reintroduced into the long arm of the cavity and rotated so as to operate in the 1st order. Under 2.6 W of incident pump power (1.8 W absorbed power) broadly

Optics EXPRESS

tunable mode-locked operation was recorded (see Visualization 1). Pulse durations varying from 240 fs to 538 fs were generated over a tuning range of 2019–2110 nm [Fig. 5(a)]. It is believed that the variation of the pulse duration across the tunability range is predominantly due to the soliton mode-locking regime where the pulse duration is inversely proportional to the intracavity pulse energy ($\tau_p \propto 1/E_p$ [30]) and thus the average output power, as can be seen from Fig. 5(a). Additionally, further increasing of the pulse duration in the 2030–2080 nm range could also be associated with the smaller modulation depth of SESAM in that region compared to the 2.1 μm region. The shortest pulse duration of 240 fs was produced at an output power of 93 mW. Figures 5(b) and 5(c) show the optical spectrum and intensity autocorrelation trace for a pulse recorded at 2090 nm, respectively A pulse duration of 245 fs (assuming a sech^2 intensity autocorrelation profile) with a corresponding optical bandwidth of 19.6 nm (FWHM) was recorded, giving a time-bandwidth product of 0.33 and indicating near-transform-limited pulse operation. In addition, monitoring of the autocorrelation traces over a 50 ps span showed no signs of multipulsing while clean RF spectra confirmed Q-switching instability free operation at a pulse repetition frequency of 114.3 MHz. This was found at all points throughout the tuning range. Mode-locked operation was self-starting and after an initial half an hour warm-up time, required for the laser diode thermalization affecting the pump beam pointing, stable and consistent performance was maintained for a number of hours.

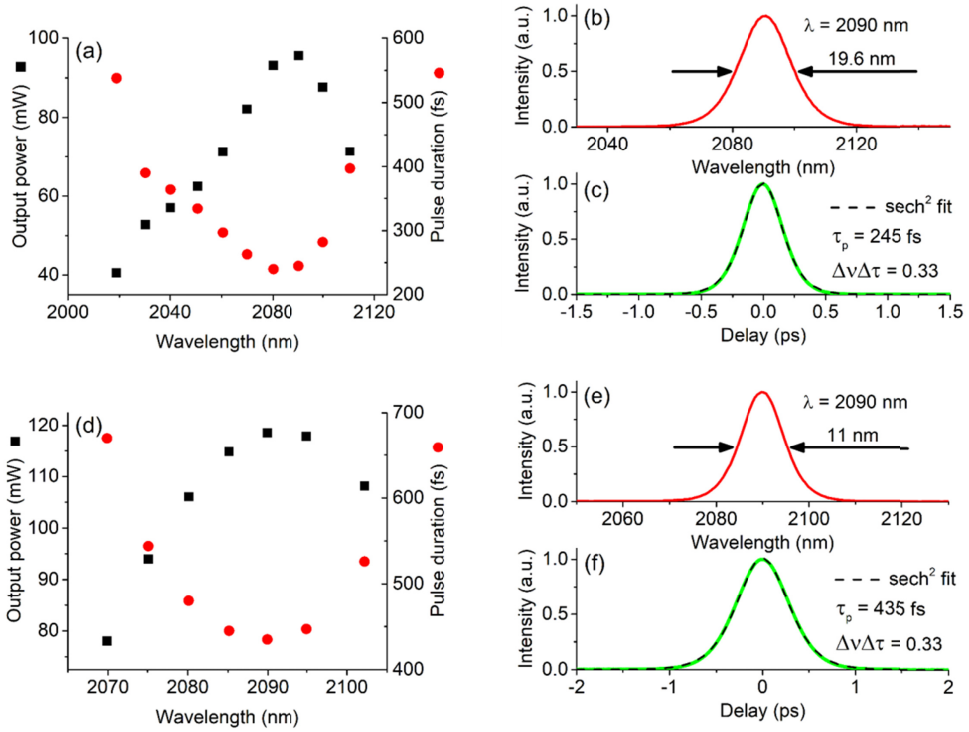

Fig. 5. (a) Tm:$LuScO_3$ mode-locked laser tuning characteristics for the 1st order of operation of the SD-BRF with the 1% output coupler (see Visualization 1). (b) and (c) show the optical spectrum and autocorrelation trace for a pulse recorded at 2090 nm, respectively. (d), (e), and (f) show the performance recorded when using the 2% output coupler and operating in the 1st order of the SD-BRF.

Rotating the BRF to operate in the 2nd order gave similar results to the 1st order in terms of tuning range and the variation of pulse duration and output power with the wavelength. However, comparably longer pulse durations (349–685 fs) were recorded over the 2025–2114

Optics EXPRESS

nm tuning range with average output powers of between 36 mW and 63 mW. This increase in pulse duration is presumed to be the result of lower output power. However, the narrower transmission bandwidth provided by the 2nd order of the SD-BRF could be an additional factor which limited optical bandwidth and duration of the generated pulses. As with the 1st order, the mode-locking stability was confirmed by examining widespan autocorrelation traces and RF spectra.

Increasing the output coupling to 2% resulted in higher average output powers but with a narrower tuning range and longer pulse durations. Operating in the 1st order, a tuning range of 2070–2102 nm was recorded, with output power and pulse durations varying from 78 fs to 119 mW and 435–670 fs, respectively [Fig. 5(d)]. It can be seen that the pulse durations and output power followed a similar profile to that seen with the 1% output coupler, with the maximum output power and minimum pulse duration found around 2090 nm. Figures 5(e) and 5(f) show the optical spectrum and intensity autocorrelation traces for a pulse recorded at 2090 nm, respectively. A pulse duration of 435 fs with an associated optical bandwidth of 11 nm were measured, giving a time-bandwidth product of 0.33. Moving to the 2nd order with the 2% output coupler gave a similar tuning range of 2072–2108 nm, with output powers varying between 74 mW and 103 mW and near-transform-limited pulses ranging from a maximum pulse duration of 811 fs to a minimum pulse duration of 563 fs. As with the 1% output coupler, clean RF spectra and widespan autocorrelation traces confirmed stable, single pulse mode-locked operation throughout the tuning range at a pulse repetition frequency of 114.3 MHz.

Only picosecond pulse durations were realized when operating in the 3rd order of the SD-BRF and using the 1% output coupler. A narrower tuning range than that recorded from the 1st or 2nd orders was observed with relatively unstable operation. No mode-locked operation was achieved when operating in the 4th order of the SD-BRF. These results can be associated with the relatively narrow optical bandwidths of the SD-BRF at higher orders that could be preventing pulse spectral broadening and stable soliton mode-locking.

It can be seen that the SD-BRF can be used as a means to not only to set the emission wavelength but also coarsely control the pulse duration of mode-locked pulses. Indeed, pulse durations of 245 fs, 363 fs, and 1 ps have been experimentally demonstrated around 2090–2095 nm for the 1st, 2nd, and 3rd orders, respectively. It was quite clear that the pulse durations increase and the corresponding optical bandwidths decrease with the higher orders. However, it is difficult to separate the SD-BRF narrowing effect from the effects of lower intracavity pulse energy when explaining the reduced bandwidth recorded with higher orders of the filter. It is believed that stable operation can be realized with higher orders but that the laser cavity parameters such as beam waists and dispersion would have to be additionally tailored for such mode-locking regimes.

4. Summary and outlook

We have demonstrated femtosecond pulses tunable over >90 nm around 2.06 μm from a diode-pumped, mode-locked Tm:$LuScO_3$ laser. Using a 1% output coupler and operating in the 1st order of the SD-BRF, tuning between 2019 nm and 2110 nm was achieved with the pulse durations varying from 240 fs to 538 fs and average output powers from 41 mW to 96 mW. Moving to the 2nd order gave a similar tuning range but with longer pulse durations of 349–685 fs. A 2% output coupler realized higher output powers over a narrower tuning range with minimum pulse durations of 435 fs and 563 fs recorded in the 1st and 2nd orders of the SD-BRF, respectively. To the best of our knowledge this is the first demonstration of a SD-BRF being used in the 2–2.1 μm region for broadband tuning of femtosecond pulses. In addition, the utilization of a SD-BRF to achieve broad femtosecond pulse tuning allows for a less complex and more robust cavity design compared with the traditionally used slit and prism pair combination.

Optics EXPRESS

Based on the demonstrated performance, it can be concluded that the mode-locked Tm:$LuScO_3$ laser could be used as a seed source for existing Ho^{3+}-doped amplifiers in the 2050–2090 nm range. In particular, the >100 mW average output power level and ~570 fs pulses ($\Delta\lambda \approx 8.5$ nm) achieved with the 2% output coupler and the 2nd order of the BRF would be particularly suitable for the narrow gain bands of Ho:YAG at 2090 nm. Additionally, when using the 1% output coupler, the gain peaks of Ho:YLF around 2050/2060 nm can be reached as well with an average mode-locked power of >50 mW. There is also potential for the Tm:$LuScO_3$ ultrafast laser source to be used as a seed for further amplification in a Tm^{3+}-doped sesquioxide gain medium, in particular Tm:Lu_2O_3 which benefits from excellent thermo-mechanical properties and broadband gain in the 2060–2080 nm range.

Funding

Engineering and Physical Sciences Research Council (EPSRC) (EP/L01596X/1); Fraunhofer UK Research Limited studentship funding.

Acknowledgments

The authors would like to thank Prof. Alan Kemp for supplying the base Mathcad script used in modelling the performance of the steeply diving birefringent filter. The research data supporting this publication can be accessed at https://doi.org/10.17630/dcad996c-1f8a-41a5-9de3-88076a318b7f .

References

1. P. A. Budni, L. A. Pomeranz, M. L. Lemons, C. A. Miller, J. R. Mosto, and E. P. Chicklis, "Efficient mid-infrared laser using 1.9-µm-pumped Ho:YAG and ZnGeP2 optical parametric oscillators," J. Opt. Soc. Am. B **17**(5), 723–728 (2000).
2. N. Leindecker, A. Marandi, R. L. Byer, K. L. Vodopyanov, J. Jiang, I. Hartl, M. Fermann, and P. G. Schunemann, "Octave-spanning ultrafast OPO with 26-61µm instantaneous bandwidth pumped by femtosecond Tm-fiber laser," Opt. Express **20**(7), 7046 (2012).
3. J. Swiderski, "High-power mid-infrared supercontinuum sources: current status and future perspectives," Prog. Quantum Electron. **38**(5), 189–235 (2014).
4. T. Popmintchev, M.-C. Chen, D. Popmintchev, P. Arpin, S. Brown, S. Ališauskas, G. Andriukaitis, T. Balčiunas, O. D. Mücke, A. Pugzlys, A. Baltuška, B. Shim, S. E. Schrauth, A. Gaeta, C. Hernández-García, L. Plaja, A. Becker, A. Jaron-Becker, M. M. Murnane, and H. C. Kapteyn, "Bright coherent ultrahigh harmonics in the keV x-ray regime from mid-infrared femtosecond lasers," Science **336**(6086), 1287–1291 (2012).
5. S. Amini-Nik, D. Kraemer, M. L. Cowan, K. Gunaratne, P. Nadesan, B. A. Alman, and R. J. D. Miller, "Ultrafast mid-IR laser scalpel: protein signals of the fundamental limits to minimally invasive surgery," PLoS One **5**(9), e13053 (2010).
6. D. M. Bubb, M. R. Papantonakis, J. S. Horwitz, R. F. Haglund, Jr., B. Toftmann, R. A. McGill, and D. B. Chrisey, "Vapor deposition of polystyrene thin films by intense laser vibrational excitation," Chem. Phys. Lett. **352**(3-4), 135–139 (2002).
7. M. Sparkes and W. M. Steen, ""Light" industry: an overview of the impact of lasers on manufacturing," in *Advances in Laser Materials Processing*, II (Woodhead Publishing, 2018).
8. K. C. Cossel, E. M. Waxman, I. A. Finneran, G. A. Blake, J. Ye, and N. R. Newbury, "Gas-phase broadband spectroscopy using active sources: progress, status, and applications," J. Opt. Soc. Am. B **34**(1), 104–129 (2017).
9. M. Hemmer, D. Sánchez, M. Jelínek, V. Smirnov, H. Jelinkova, V. Kubeček, and J. Biegert, "2-µm wavelength, high-energy Ho:YLF chirped-pulse amplifier for mid-infrared OPCPA," Opt. Lett. **40**(4), 451–454 (2015).
10. L. von Grafenstein, M. Bock, U. Griebner, and T. Elsaesser, "High-energy multi-kilohertz Ho-doped regenerative amplifiers around 2 µm," Opt. Express **23**(11), 14744–14752 (2015).
11. L. von Grafenstein, M. Bock, D. Ueberschaer, U. Griebner, and T. Elsaesser, "Picosecond 34 mJ pulses at kHz repetition rates from a Ho:YLF amplifier at 2 µm wavelength," Opt. Express **23**(26), 33142–33149 (2015).
12. L. von Grafenstein, M. Bock, D. Ueberschaer, U. Griebner, and T. Elsaesser, "Ho:YLF chirped pulse amplification at kilohertz repetition rates - 4.3 ps pulses at 2 µm with GW peak power," Opt. Lett. **41**(20), 4668–4671 (2016).
13. L. von Grafenstein, M. Bock, G. Steinmeyer, U. Griebner, and T. Elsaesser, "Taming chaos: 16 mJ picosecond Ho: YLF regenerative amplifier with 0.7 kHz repetition rate," Laser Photonics Rev. **10**(1), 123–130 (2016).
14. P. Li, A. Ruehl, C. Bransley, and I. Hartl, "Low noise, tunable Ho:fiber soliton oscillator for Ho:YLF amplifier seeding," Laser Phys. Lett. **13**(6), 65104 (2016).
15. M. Hinkelmann, D. Wandt, U. Morgner, J. Neumann, and D. Kracht, "Mode-locked Ho-doped laser with

Optics EXPRESS

subsequent diode-pumped amplifier in an all-fiber design operating at 2052 nm," Opt. Express **25**(17), 20522–20529 (2017).
16. M. Hinkelmann, B. Schulz, D. Wandt, U. Morgner, M. Frede, J. Neumann, and D. Kracht, "Millijoule-level, kilohertz-rate, CPA-free linear amplifier for 2 µm ultrashort laser pulses," Opt. Lett. **43**(23), 5857–5860 (2018).
17. M. Hinkelmann, D. Wandt, U. Morgner, J. Neumann, and D. Kracht, "High repetition rate, µJ-level, CPA-free ultrashort pulse multipass amplifier based on Ho:YLF," Opt. Express **26**(14), 18125–18130 (2018).
18. C. Kränkel, "Rare-earth-doped sesquioxides for diode-pumped high-power lasers in the 1-, 2-, and 3-µm spectral range," IEEE J. Sel. Top. Quantum Electron. **21**(1), 250 (2015).
19. A. Schmidt, P. Koopmann, G. Huber, P. Fuhrberg, S. Y. Choi, D.-I. Yeom, F. Rotermund, V. Petrov, and U. Griebner, "175 fs Tm:Lu2O3 laser at 2.07 µm mode-locked using single-walled carbon nanotubes," Opt. Express **20**(5), 5313–5318 (2012).
20. A. A. Lagatsky, O. L. Antipov, and W. Sibbett, "Broadly tunable femtosecond Tm:Lu2O3 ceramic laser operating around 2070 nm," Opt. Express **20**(17), 19349–19354 (2012).
21. A. A. Lagatsky, P. Koopmann, O. L. Antipov, C. T. A. Brown, G. Huber, and W. Sibbett, "Femtosecond pulse generation with Tm-doped sesquioxides," in *2013 Conference on Lasers & Electro-Optics Europe & International Quantum Electronics Conference CLEO EUROPE/IQEC* (IEEE, 2013), p. CA_6_3.
22. Y. Wang, W. Jing, P. Loiko, Y. Zhao, H. Huang, X. Mateos, S. Suomalainen, A. Härkönen, M. Guina, U. Griebner, and V. Petrov, "Sub-10 optical-cycle passively mode-locked Tm:(Lu2/3Sc1/3)2O3 ceramic laser at 2 µm," Opt. Express **26**(8), 10299–10304 (2018).
23. A. A. Lagatsky and J.-M. Hopkins, "Diode-pumped femtosecond Tm-doped Lu2O3 ceramic laser," in *Laser Congress 2016 (ASSL, LSC, LAC)* (Optical Society of America, 2016), p. JTu2A.5.
24. N. K. Stevenson, C. T. A. Brown, J.-M. Hopkins, M. D. Dawson, C. Kränkel, and A. A. Lagatsky, "Diode-pumped femtosecond Tm^{3+}-doped LuScO3 laser near 2.1 µm," Opt. Lett. **43**(6), 1287–1290 (2018).
25. B. Stormont, A. J. Kemp, I. G. Cormack, B. Agate, C. T. A. Brown, W. Sibbett, and R. Szipöcs, "Broad tunability from a compact, low-threshold Cr:LiSAF laser incorporating an improved birefringent filter and multiple-cavity Gires-Tournois interferometer mirrors," J. Opt. Soc. Am. B **22**(6), 1236–1243 (2005).
26. U. Demirbas, J. Wang, G. S. Petrich, S. Nabanja, J. R. Birge, L. A. Kolodziejski, F. X. Kärtner, and J. G. Fujimoto, "100-nm tunable femtosecond Cr:LiSAF laser mode locked with a broadband saturable Bragg reflector," Appl. Opt. **56**(13), 3812–3816 (2017).
27. U. Demırbas, "Off-surface optic axis birefringent filters for smooth tuning of broadband lasers," Appl. Opt. **56**(28), 7815–7825 (2017).
28. K. Naganuma, G. Lenz, and E. P. Ippen, "Variable bandwidth birefringent filter for stable femtosecond lasers," IEEE J. Quantum Electron. **28**(10), 2142–2150 (1992).
29. A. A. Lagatsky, X. Han, M. D. Serrano, C. Cascales, C. Zaldo, S. Calvez, M. D. Dawson, J. A. Gupta, C. T. A. Brown, and W. Sibbett, "Femtosecond (191 fs) NaY(WO4)2 Tm,Ho-codoped laser at 2060 nm," Opt. Lett. **35**(18), 3027–3029 (2010).
30. U. Keller, "2.1 Ultrafast solid-state lasers," in *Laser Physics and Applications* (Springer-Verlag, 2007).